

X-ray powder diffraction profile refinement of synthetic hercynite

RODERICK J. HILL

CSIRO Division of Mineral Chemistry
P.O. Box 124, Port Melbourne
Victoria 3207 Australia

Abstract

A full profile X-ray powder diffraction structure refinement has been completed on a sample of synthetic hercynite, FeAl_2O_4 , using graphite monochromatized $\text{CuK}\alpha$ step-scan data ($2\theta_{\text{max}} = 140^\circ$) and a flexible profile shape of the pseudo-Voigt type. The most satisfactory convergence was achieved at $R_{\text{wp}} = 0.0781$ and $R_{\text{B}} = 0.0125$ using fully ionized atomic scattering factors and a peak shape parameter of the form $\epsilon = 0.233(17) + 0.0055(3)2\theta$: the individual peak shapes vary from 33.7% Lorentzian to 99.8% Lorentzian character as 2θ increases. The derived structural parameters at 20°C are: $a = 8.15579(6)\text{\AA}$, i (inversion) = $0.163(5)$, $x(0) = 0.2633(2)$, $B = 0.56(3)$, $0.44(3)$ and $1.07(5)\text{\AA}^2$ for the tetrahedral (Fe), octahedral (Al) and oxygen atoms, respectively. Calculated values for a and x based on the ionic model and $i = 0.163$ are in good agreement with the refined values.

Introduction

The crystal chemistry of the spinel hercynite, FeAl_2O_4 , is of considerable interest to mineralogists and materials scientists because of its importance in metamorphic petrology (Osborne et al., 1981; Rumble, 1976; Turnock and Eugster, 1962; Palache et al., 1944, p.687), ceramics (Mason and Bowen, 1981; Meyers et al., 1980; Baldwin, 1955) and device applications (Zhukovskaya et al., 1980; Dehe et al., 1975; Hoffmann and Fischer, 1956). However, the detailed crystal structure of this phase (in particular its cation distribution) remains uncertain, primarily because pure hercynite is rarely, if ever, encountered in nature (Turnock and Eugster, 1962; Palache et al., 1944, p. 692) and because synthetic hercynites in the $\text{FeO}-\text{Fe}_2\text{O}_3-\text{Al}_2\text{O}_3$ system often contain significant levels of non-stoichiometry arising from valence state variations, interstitial atoms and oxygen atom vacancies (Mason and Bowen, 1981; Halloran and Bowen, 1980). Indeed, many of the natural "hercynites" documented in the literature are more properly classified as members of the $\text{MgAl}_2\text{O}_4-\text{FeAl}_2\text{O}_4$ (pleonaste) or $\text{Fe}_3\text{O}_4-\text{FeAl}_2\text{O}_4$ solid solution series.

A compound AB_2X_4 with the spinel structure crystallizes in space group $Fd\bar{3}m$ with the A cation in site $8a$ at $(1/8\ 1/8\ 1/8)$, the B cation in site $16d$ at $(1/2\ 1/2\ 1/2)$, and the anion in site $32e$ at (xxx) , when the origin is at $16d$ (Bragg, 1915; Hafner, 1960; Blass, 1964; Hill et al., 1979). The structure then requires only three parameters (excluding thermal vibration coefficients) to describe its atomic arrangement completely: the unit cell size, a , the anion positional coordinate, x , and the cation ordering, or

inversion parameter, i . For $i = 0$ and 1 , respectively, the spinel has the so-called normal, $\text{A}[\text{B}_2]\text{X}_4$, and inverse, $\text{B}[\text{AB}]\text{X}_4$, cation distributions, where the ions indicated in parenthesis are in octahedral coordination by X, and the remaining ions (including X) are in tetrahedral coordination. Intermediate cation distributions may be represented as $(\text{A}_{1-i}\ \text{B}_i)[\text{A}_i\ \text{B}_{2-i}]\text{X}_4$.

For those phases which have been described as FeAl_2O_4 in the literature the unit cell dimensions have been determined to lie in the range $8.08-8.16\text{\AA}$ (Segnit, 1984). This rather large range of values suggests that not all of the samples are stoichiometric and/or they contain some Fe^{3+} or other cation. The oxygen coordinate has been determined twice, yielding values of "about" 0.265 (Barth and Posnjak, 1932) and $0.2635(1)$ (Roth, 1964). Estimates of the distribution of Fe^{2+} over the octahedral and tetrahedral sites obtained from diffraction and Mössbauer measurements vary between $i = 0.0$ and 0.25 (Osborne et al., 1981; Dickson and Smith, 1976; Yagnik and Mathur, 1968; Barth and Posnjak, 1932; Roth, 1964).

The present study of synthetic hercynite was initiated (1) in order to accurately characterize the crystal structure of this important phase, and (2) as part of a broader investigation into the application of full-profile Rietveld-type powder diffraction structure refinement methods and detailed peak-shape modelling in the case of two-wavelength X-ray data.

Experimental

The sample of FeAl_2O_4 used in the present study was synthesized in an evacuated silica tube at 1050°C for 4 days using a stoichiometric mixture of Fe, Fe_2O_3 and $\gamma\text{-Al}_2\text{O}_3$ followed by

Table 1. Crystal structure refinement results for hercynite

Parameter	X-ray profile (present study)	Neutron integrated (Roth, 1964)
a (Å)	8.15579(6)*	8.152
$B(\text{tet.})$ (Å ²)	0.56(3)	0.82
$B(\text{oct.})$ (Å ²)	0.44(3)	
$B(O)$ (Å ²)	1.07(5)	
$x(O)$	0.2633(2)	0.2635(1)
Inversion, i	0.163(5)	0.154(10)
Scale	0.001196(6)	
U^\dagger	0.0154(11)	
V	-0.0141(21)	
W	0.0296(8)	
2θ zero	-0.0857(5)	
Asymmetry**	0.96(6)	
ϵ ††	0.233(17)	
ϵ_0	0.0055(3)	
No. of observations	1207	14
$R_p^\#$	0.0568	-
R_{wp}	0.0781	-
R_B	0.0125	0.010

* Numbers in parenthesis are the esd's in terms of the least significant figure to the left.

† Coefficient in the expression: $\text{FWHM}^2 = U \tan^2 \theta + V \tan \theta + W$ (Caglioti et al., 1958).

** As defined by Rietveld (1969).

†† Coefficient in the expression: pseudo-Voigt $\epsilon = \epsilon_0 + \epsilon_1 \cdot 2\theta$.

Agreement indices defined by Young and Prince (1982); R_p is roughly equivalent to twice the conventional R value obtained from integrated peak structure refinements.

annealing at 850°C for 5 days (pers. comm., V.J. Wall, Dept. of Earth Sciences, Monash University). The maximum amount of Fe^{3+} is estimated from Mössbauer measurements to be about 4% of the total Fe content (personal communication from W.A. Dollase, Dept. of Earth Sciences, UCLA to V.J. Wall).

The hercynite powder was back-pressed into a standard aluminium holder and mounted in a Philips PW1050 diffractometer equipped with a PW1710 automatic step-scanning system and a diffracted-beam curved graphite monochromator. Intensity measurements were made at 20°C at intervals of 0.04°2 θ over the range 17–140°2 θ using $\text{CuK}\alpha$ radiation and a step counting time of 5 s. The X-ray tube was operated at 45 kV and 26 mA, with 1° divergence and receiving slits. These conditions allowed the collection of profile data for a total of 72 Bragg reflections with background counts in the range 150–1200 and a maximum peak intensity of 45,000 counts. Dead-time corrections were applied automatically during data collection.

Structure refinement

The least-squares structure refinements were undertaken with the full-profile, Rietveld-type, program DBW3.2 (Rietveld, 1969; Wiles and Young, 1981) locally modified to include the application of a 2 θ -variable profile shape function of the form:

$$\epsilon = \epsilon_0 + \epsilon_1 \cdot 2\theta$$

where ϵ is the fractional Lorentzian character of the peaks in the pseudo-Voigt function (Hindeleh and Johnson, 1978). This program can accept X-ray data obtained from a conventional diffractometer since it allows the simultaneous refinement of two wavelengths (i.e., α_1 and α_2) if their intensity ratio is known (2:1 in the present case). The weight assigned to the intensity observed at each step i in the pattern is $W_i = 1/Y_{i0}$ and the function minimized in the least-squares procedure is $W_i(Y_{i0} - Y_{ic})^2$, where Y_{i0} and Y_{ic} are the observed and calculated intensities, respectively.

The refined quantities were a scale factor, the pseudo-Voigt profile shape parameters ϵ_0 (and ϵ_1 in the final refinement cycles), a 2 θ zero parameter, a peak full width at half maximum (FWHM) function (of the form: $\text{FWHM}^2 = U \tan^2 \theta + V \tan \theta + W$; Caglioti et al. 1958) calculated for 3.5 half-widths on either side of the peak position, a peak asymmetry parameter (Rietveld, 1969) for reflections with $d > 2.2\text{Å}$, the unit cell constant, a , the x coordinate of the oxygen atom, $x(O)$, isotropic thermal parameters, B , for all three atoms, and a site occupancy parameter, i , arranged to model cooperative cation disorder over both the octahedral and tetrahedral positions. The background was evaluated by linear interpolation between 18 points selected at roughly 7° intervals in 2 θ over the entire pattern. Note that when the background is estimated by interpolation, rather than by refinement, only those data points within 3.5% FWHM on either side of the peak positions are included in the profile refinement. The number of "observations" is, therefore, reduced from 3076 to 1207. Scattering factors (including the anomalous dispersion coefficients) for Fe, Fe^{2+} , Al, Al^{3+} , O and O^{1-} were obtained from Ibers and Hamilton (1974) and that of O^{2-} was obtained from Hovestreydt (1983). An experimentally determined value of 0.91 was used for the monochromator polarization correction.

The refinements were initiated using $a = 8.159\text{Å}$, $x = 0.265$, $\epsilon_0 = 0.5$, $\epsilon_1 = 0.0$, $i = 0$, $B(\text{tet.}) = B(\text{oct.}) = 0.5\text{Å}^2$, $B(O) = 1.0\text{Å}^2$, and a scale factor and half-width parameters estimated by inspection of the observed diffraction pattern. There was no evidence for the presence of preferred orientation although several very small peaks due to a contaminating phase were observed. Refinement was continued until the parameter shifts in the last cycle were all less than one quarter of their associated esd's. Combinations of scattering factors corresponding to neutral, half-ionized and fully-ionized atoms were carried to convergence separately. The pseudo-Voigt ϵ_1 parameter was only released for the last few cycles of full-matrix refinement. The complete set of results for the best-fit model are given in Table 1 where they may be compared to the integrated intensity neutron powder diffraction results of Roth (1964). The raw digital intensity data have been deposited,¹ but a plot of the observed, calculated and difference profiles for the final refinement is given in Figure 1. A list of observed and calculated integrated

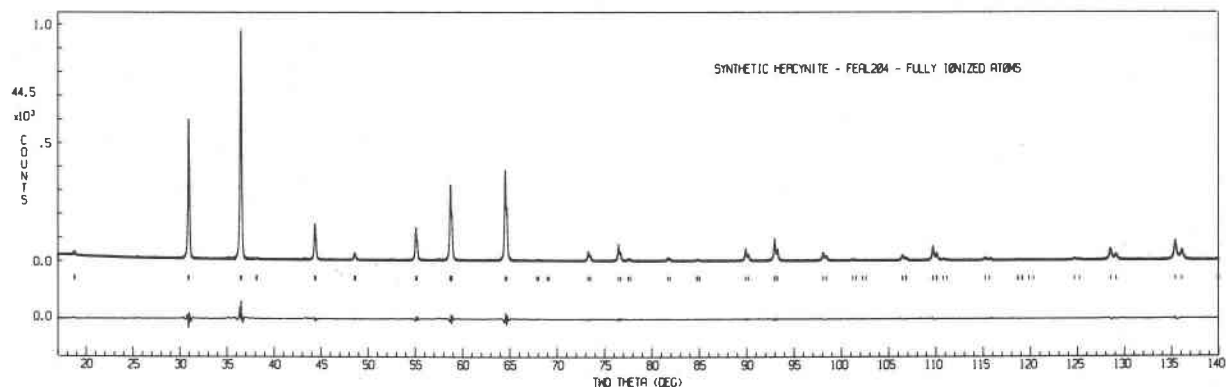


Fig. 1. Observed, calculated and difference X-ray powder diffraction profiles for synthetic hercynite. The observed data are indicated by plus signs and the calculated profile by the continuous line overlying them. The short vertical lines below the pattern represent the positions of all possible Bragg reflections and the lower curve shows the value of $(Y_{io} - Y_{ic})$ at each step.

peak intensities, together with their d -spacings, for all peaks with intensities greater than 1% of the maximum is given in Table 2.

With the profile and structural parameters set equal to the values obtained from the best-fit model the 12 most intense Bragg peaks were considered individually in refinements of the scale factor, 2θ zero, half-width W term, and pseudo-Voigt ϵ_0 parameter. The resultant peak

widths and ϵ_0 parameters are plotted as a function of 2θ in Figure 2.

Discussion

Structural parameters

Refinement of the model with fully-ionized atom scattering factors produced a slightly better fit between the observed and calculated profiles, as measured by R_p and R_{wp} , than the neutral and half-ionized models. However, none of the parameters, including the relatively sensitive thermal vibration parameters, B , and inversion parameter, i , were affected by more than 1.5 combined esd's by the different form factor models.

The mean isotropic thermal vibration parameter of 0.82\AA^2 is in reasonable agreement (by X-ray powder diffraction standards) with the single value 0.99(5) determined for hercynite by Roth (1964) (Table 1), with the values 0.56(4) and $0.3(1)\text{\AA}^2$ determined for synthetic

Table 2. Observed and calculated integrated peak intensities and d -spacings for hercynite reflections with intensities greater than 1% of the maximum calculated value

h	k	l	$d(\text{\AA})$	I_{obs}	I_{calc}
1	1	1	4.709	1.1	1.1
0	2	2	2.884	57.4	57.9
1	1	3	2.459	102.6	100.0
0	0	4	2.039	17.2	17.2
1	3	3	1.871	3.5	3.4
2	2	4	1.665	16.8	17.0
1	1	5	1.570	41.4	41.5
3	3	3			
0	4	4	1.442	49.3	49.9
0	2	6	1.290	5.7	5.6
3	3	5	1.241	10.0	9.8
2	2	6	1.230	1.4	1.3
4	4	4	1.177	1.8	1.7
2	4	6	1.090	8.0	7.8
1	3	7	1.062	15.1	14.9
3	5	5			
0	0	8	1.019	6.2	6.1
0	6	6	0.9612	4.5	4.4
2	2	8			
1	5	7	0.9418	11.3	10.9
5	5	5			
2	6	6	0.9355	1.3	1.2
0	4	8	0.9119	2.3	2.2
4	6	6	0.8694	1.8	1.7
1	3	9	0.8550	12.6	12.3
4	4	8	0.8324	22.2	22.0

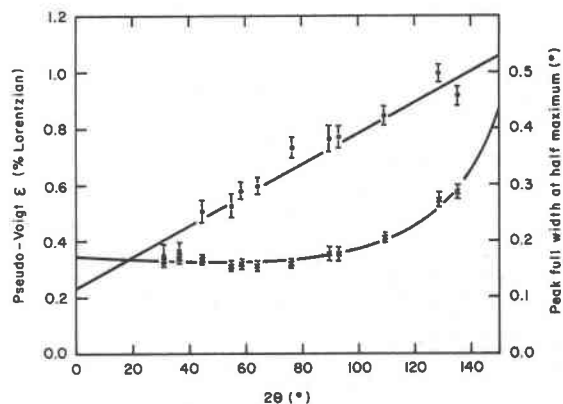


Fig. 2. Variation of the individual peak pseudo-Voigt parameters (solid circles) and peak full widths at half maximum (crosses) with 2θ for the 12 most intense peaks in the X-ray diffraction pattern of hercynite. The peak width and shape relationships determined by refinement of the entire pattern are shown as continuous lines.

Table 3. Interatomic distances and angles for hercynite

AO ₄ tetrahedron: A = Fe _{0.84} Al _{0.16}		
A-O	[×4]	1.954(2) Å
O-A-O	[×6]	109.47(10)°
O-O	[×6]	3.190(3) Å
BO ₆ octahedron: B = Al _{1.84} Fe _{0.16}		
B-O	[×6]	1.937(2) Å
O-O	[×6]	2.577(3) Å shared edge
O'-O'	[×6]	2.892(1) Å unshared edge
O-B-O	[×6]	83.41(7)°
O'-B-O'	[×6]	96.59(7)°
OAB ₃ polyhedron		
O-A	[×1]	1.954(2) Å
O-B	[×3]	1.937(2) Å
A-B	[×3]	3.381(0) Å
B-B	[×3]	2.884(0) Å across shared edge
A-O-B	[×3]	120.72(8)°
B-O-B	[×3]	96.23(7)°
Shortest A-A = 3.532 Å		

MgAl₂O₄ and ZnAl₂O₄, respectively, from neutron powder diffraction data (Fischer, 1967), and with the value 1.0(2)Å² determined for synthetic Fe₃O₄ from neutron single crystal data (Hamilton, 1958).

The inversion parameter value of 0.163(5), corresponding to the cation distribution



lies in the middle of the range $i = 0.0-0.25$ determined for hercynite in the past, and is very close to the value 0.154(10) obtained by Roth (1964) (Table 1). The large range exhibited by the previous X-ray and Mössbauer determinations is probably a reflection of the difficulty in estimating the areas of weak shoulder peaks in the Mössbauer spectra and/or problems associated with non-stoichiometry and phase impurity in the earlier samples.

The refined positional parameter for oxygen, 0.2633(2), is very close to the value obtained by Roth (1964), and the unit cell size, 8.15579(6)Å, falls at the upper end of the range of literature values clustering around 8.16Å (Segnit, 1984). The a and x values determined in the present study may be compared with values of 0.2640 and 8.136Å calculated with the relationships of Hill et al. (1979) using the observed inversion parameter and the spinel-optimized cation radii of O'Neill and Navrotsky (1983). Note that the lattice parameter determined from the profile refinement, even allowing for the cubic symmetry and well crystallized nature of the sample used, is unusually precise because of the requirement that the calculated and observed profiles match all along their steep sides as well as at the peak center.

The bonding dimensions resulting from the determined a and x values are summarized in Table 3. As expected for a spinel with $x > 0.25$, the three edges shared between adjacent octahedra are shorter (in this case by 0.32Å)

than the unshared ones, and the valence angles are distorted 6.6° from their ideal values. The tetrahedron retains its $\bar{4}3m$ symmetry with a bond length expanded by 0.19Å over the value corresponding to ideal close packing of the anions ($x = 0.25$), while the octahedron has $\bar{3}m$ symmetry with bond lengths decreased by 0.10Å from their ideal values. The bond lengths are consistent with values calculated using the observed site populations (Table 1) and the effective ionic radii of O²⁻, Fe²⁺ and Al³⁺ (O'Neill and Navrotsky, 1983).

Parameter esd's

The subject of the accuracy of parameter esd's determined in profile structure refinements has been extensively debated in the recent literature (Scott, 1983; Cooper, 1982; Cooper et al., 1981; Hewat and Sabine, 1981; Prince, 1981; Bacon and Lisher, 1980; Prince, 1980; Sakata and Cooper, 1979). The general conclusion is that profile refinement esd's may be underestimated by a factor of 2 or so compared to the results obtained from integrated intensity refinements when the model, including both the structure and the profile parts, is not correct. However, in cases, like the present study, where the diffraction peak profile shape is itself a refineable parameter, it may be expected that the esd's of the structural parameters more closely reflect the true distribution about their mean values. Indeed, while the major contributions to the least-squares residual do lie under the peaks in Figure 1, the satisfactory value for R_{wp} indicates that the peak shape model is reasonable, by X-ray standards, in the present case.

Comparison of the profile refinement results obtained in the present X-ray study with those obtained in the integrated intensity neutron data refinement of Roth (1964) (Table 1) demonstrates that the values of the parameters themselves are unaffected by the different refinement methods. Moreover, the esd's determined for all parameters common to both studies are of very similar magnitude, lending support to the estimates obtained in the profile refinement.

Peak shape and half-width

The power of the pseudo-Voigt profile function is that it allows a continuous variation in shape from pure Lorentzian or Cauchy ($\epsilon = 1.0$) through to a pure Gaussian ($\epsilon = 0.0$). Indeed, Young and Wiles (1982) have concluded that the pseudo-Voigt and Pearson VII (Hall et al., 1977) peak shape functions are consistently the best options for Rietveld refinements of both X-ray and neutron diffraction data.

In the present study the best fit between the observed and calculated peak shapes was achieved by varying the shape linearly as a function of 2θ (Fig. 2). At the low 2θ end of the diffraction pattern the peaks have about 34% Lorentzian character, whereas at the high 2θ end they approximate to a pure Lorentzian form. This indicates that for a given FWHM, a greater proportion of the integrated intensity lies in the peak tails as the diffraction

angle increases. A similar increase in Lorentzian character has been observed in other X-ray and neutron diffraction studies undertaken in our laboratories (Hill and Howard, in preparation) and in the case of Fe_3O_4 neutron diffraction data by Santoro and Prince (1980), who suggested that the variation in shape could be related to structural distortions and/or the presence of particular distributions of crystallite sizes within the sample analyzed.

For hercynite the neglect of the peak shape dependence on 2θ not only results in a significantly poorer fit between the observed and calculated peak profiles ($R_{wp} = 0.090$ compared to 0.078), but also results in a systematic overestimation of the atomic thermal vibration parameters. However, in spite of this, none of the structural parameters are affected by more than two combined standard deviations.

When individual strong peaks are isolated from the pattern as a whole and refinements are made of the individual ϵ_0 and W parameters, the resultant FWHM values lie close to the relationship between half-width and 2θ determined from the overall U , V and W parameters (Fig. 2). The similarity between the form of the individual peak width variation with 2θ and the variation produced by the Caglioti et al. (1958) formula not only indicates that the Caglioti et al. relationship between half-width and 2θ is satisfactory for X-ray data, but also shows that the crystallites are relatively isotropic in shape and unstrained. The systematic variation in the individual ϵ values can not, therefore, be related to the presence of either of these properties in the sample. The only parameter with which ϵ shows even a modest correlation coefficient (0.42) is the peak width parameter W and this relationship is to be expected.

The source of the profile shape change therefore remains undetermined. Possible explanations could involve the effect of thermal diffuse scattering, changes in the diffractometer resolution function, or variable crystallite size contributions to different parts of the pattern. In any event, if the presence of peak shape variations within powder patterns proves to be widespread it is clear that a 2θ -dependence for the profile shape function should be routinely implemented in the profile refinement procedure. For hercynite the function $\epsilon = \epsilon_0 + \epsilon_1 \cdot 2\theta$ adequately accounts for the shape variation (Fig. 2), but this may not be the case for other samples.

Acknowledgments

I am grateful to my colleagues I. C. Madsen for assistance during data collection and Dr E. R. Segnit for discussions about natural hercynite crystal chemistry, and to Dr H. G. Scott of the CSIRO Division of Materials Science for his constructive criticism of an early version of the manuscript.

References

Bacon, G. E. and Lisher, E. J. (1980) A neutron powder diffraction study of deuterated α - and β -resorcinol. *Acta Crystallographica*, B36, 1908–1916.

- Baldwin, B. G. (1955) The formation and decomposition of hercynite ($\text{FeO} \cdot \text{Al}_2\text{O}_3$). *Journal of the Iron and Steel Institute*, 179, 142–146.
- Barth, F. W. and Posnjak, E. (1932) Spinel structures: with and without variate atom equipoints. *Zeitschrift für Kristallographie*, 82, 325–341.
- Blass, G. (1964) Crystal chemistry and some magnetic properties of mixed metal oxides with spinel structure. *Philips Research Reports*, Suppl. no. 3, 1–139.
- Bragg, W. H. (1915) The structure of the spinel group of crystals. *Philosophical Magazine*, 30, 305–315.
- Caglioti, G., Paoletti, A. and Ricci, F. P. (1958) Choice of collimators for a crystal spectrometer for neutron diffraction. *Nuclear Instruments*, 3, 223–228.
- Cooper, M. J. (1982) The analysis of powder diffraction data. *Acta Crystallographica*, A38, 264–269.
- Cooper, M. J., Rouse, K. D., and Sakata, M. (1981) An alternative to the Rietveld profile refinement method. *Zeitschrift für Kristallographie*, 157, 101–117.
- Dehe, G., Seidel, B., Melzer, K., and Michalk, C. (1975) Determination of a cation distribution model of the spinel system $\text{Fe}_{3-x}\text{Al}_x\text{O}_4$. *Physica Status Solidi (a)*, 31, 439–447.
- Dickson, B. L. and Smith, G. (1976) Low-temperature optical absorption and Mössbauer spectra of staurolite and spinel. *Canadian Mineralogist*, 14, 206–215.
- Fischer, P. (1967) Neutronenbeugungsuntersuchung der Strukturen von MgAl_2O_4 - und ZnAl_2O_4 -Spinnellen, in Abhängigkeit von der Vorgeschichte. *Zeitschrift für Kristallographie*, 124, 275–302.
- Hafner, S. (1960) Metalloxyde mit Spinnellstruktur. *Schweizerische Mineralogische und Petrographische Mitteilungen*, 40, 207–243.
- Hall, M. M., Veeraraghavan, V. G., Rubin, H., and Winchell, P. G. (1977) The approximation of symmetric X-ray peaks by Pearson type VII distributions. *Journal of Applied Crystallography*, 10, 66–68.
- Halloran, J. W. and Bowen, H. K. (1980) Iron diffusion in iron-aluminate spinels. *Journal of the American Ceramic Society*, 63, 58–65.
- Hamilton, W. C. (1958) Neutron diffraction investigation of the 119°K transition in magnetite. *Physical Review*, 110, 1050–1057.
- Hewat, A. W. and Sabine, T. M. (1981) Profile refinement of single crystal and powder data: the accuracy of crystallographic parameters. *Australian Journal of Physics*, 34, 707–712.
- Hill, R. J., Craig, J. R., and Gibbs, G. V. (1979) Systematics of the spinel structure type. *Physics and Chemistry of Minerals*, 4, 317–339.
- Hindeleh, A. M. and Johnson, D. J. (1978). Crystallinity and crystallite size measurement in polyamide and polyester fibres. *Polymer*, 19, 27–32.
- Hoffman, A. and Fischer, W. A. (1956) Bildung des Spinells $\text{FeO} \cdot \text{Al}_2\text{O}_3$ und seiner Mischkristalle mit Fe_3O_4 und Al_2O_3 . *Zeitschrift für Physikalische Chemie, Neue Folge*, 7, 80–90.
- Hovestreydt, E. (1983) On the atomic scattering factor for O^{2-} . *Acta Crystallographica*, A39, 268–269.
- Ibers, J. A. and Hamilton, W. C. (Eds.) (1974) *International Tables for X-ray Crystallography*, Vol. IV, Revised and Supplementary Tables to Volumes II and III. Kynoch, Birmingham.
- Mason, T. O. and Bowen, H. K. (1981) Cation distribution and defect chemistry of iron-aluminate spinels. *Journal of the American Ceramic Society*, 64, 86–90.

- Meyers, C. E., Mason, T. O., Petuskey, W. T., Halloran, J. W., and Bowen, H. K. (1980) Phase equilibria in the system Fe–Al–O. *Journal of the American Ceramic Society*, 63, 659–663.
- O'Neill, H. St. C. and Navrotsky, A. (1983) Simple spinels: crystallographic parameters, cation radii, lattice energies, and cation distribution. *American Mineralogist*, 68, 181–194.
- Osborne, M. D., Fleet, M. E., and Bancroft, G. M. (1981) Fe²⁺–Fe³⁺ ordering in chromite and Cr-bearing spinels. *Contributions to Mineralogy and Petrology*, 77, 251–255.
- Palache, C., Berman, H., and Frondel, C. (1933) *Dana's System of Mineralogy*, Seventh ed. Wiley, New York.
- Prince, E. (1980) Estimates of standard deviations in Rietveld powder refinement. NBS Technical Note 1142, US Department of Commerce/National Bureau of Standards, 20–23.
- Prince, E. (1981) Comparison of profile and integrated-intensity methods in powder refinement. *Journal of Applied Crystallography*, 14, 157–159.
- Rietveld, H. M. (1969) A profile refinement method for nuclear and magnetic structures. *Journal of Applied Crystallography*, 2, 65–71.
- Roth, W. L. (1964) Magnetic properties of normal spinels with only A-A interactions. *Journal de Physique (Paris)*, 25, 507–515.
- Rumble, D. III (Ed.) (1976) *Oxide Minerals. Short Course Notes, Vol. 3*, Mineralogical Society of America, Washington, D.C.
- Sakata, M. and Cooper, M. J. (1979) An analysis of the Rietveld profile refinement method. *Journal of Applied Crystallography*, 12, 554–563.
- Santoro, A. and Prince, E. (1980) Use of the Pearson type VII distribution in crystal structure refinements by the profile fitting method. NBS Technical Note 1142, US Department of Commerce/National Bureau of Standards, 8–19.
- Scott, H. G. (1983) The estimation of standard deviations in powder diffraction Rietveld refinements. *Journal of Applied Crystallography*, 16, 159–163.
- Segnit, E. R. (1984) Ferroan spinel from the Harts Ranges, Northern Territory, Australia. *Australian Mineralogist*, 45, 259–260.
- Turnock, A. C. and Eugster, H. P. (1962) Fe–Al oxides: phase relationships below 1000°C. *Journal of Petrology*, 3, 533–565.
- Wiles, D. B. and Young, R. A. (1981) A new computer program for Rietveld analysis of X-ray powder diffraction patterns. *Journal of Applied Crystallography*, 14, 149–151.
- Yagnik, C. M. and Mathur, M. (1968) *Journal of Physics C (Proceedings Physics Society)* 1, 469–472.
- Young, R. A., Prince, E., and Sparks, R. A. (1982) Suggested guidelines for the publication of Rietveld analyses and pattern decomposition studies. *Journal of Applied Crystallography*, 15, 357–359.
- Young, R. A. and Wiles, D. B. (1982) Profile shape functions in Rietveld refinements. *Journal of Applied Crystallography*, 15, 430–438.
- Zhukovskaya, T. N., Camokhvalova, O. L., Bushueva, E. V., and Chichagov, A. V. (1980) Hydrothermal synthesis and study of some physical properties of spinels in the composition Mg_{1-x}Fe_xAl₂O₄. *Zapiski Vsesoyuznogo Mineralogicheskogo Obshchestva*, 109, 367–369.

*Manuscript received, September 14, 1983;
accepted for publication, May 1, 1984.*